List of Figures **page**

List of Tables **page**

List of Equations **page**

Chapter 1 - Background

1.1 - Project Overview and Scope

Differential camber is a common occurrence among prestress concrete beams. Differential camber, with respect to this project, is defined as a variance of midspan camber for pretensioned concrete bridge girders designed to have identical camber. Currently, differential camber is mitigated with various techniques such as casting variable depth haunches over girders. The cost of modifying forms and pouring additional concrete to account for the elevation differences between girders can be significant for a large project. Differential camber also makes it more difficult to use precast deck panels, which could speed construction of bridges and buildings. The elimination of differential camber could maximize the potential of box girders and deck bulb-tee's by providing a complete precast superstructure, eliminating the delay of forming, casting and curing full width decks in place, enabling rapid construction that even composite steel could not compete with. Eliminating differential camber should provide an overall cost savings in labor and accelerated construction scheduling.

Developing criteria of camber control lends itself to dividing camber into two stages, initial and long-term. Properties of the concrete section such as moment of inertia, self-weight and Young's (Elastic) Modulus contribute to initial camber. Also steel properties such as jacking force, relaxation, elastic shortening loss and temperature effects can impact initial camber. Long-term camber is largely controlled by creep and shrinkage of concrete, and relaxation of steel, and to a lesser degree an increase in compressive strength and modulus of elasticity. For a given project it is reasonable to assume that camber growth will be the same for beams made using the same mix design, type and placement of steel, and exposed to reasonably similar environmental conditions. Below is an excerpt from Ohio DOT regarding camber in bridge girders.

"Phased construction can cause unique problems with camber. Camber is time dependent: as the members get older they will gain camber. If all beams are manufactured for a bridge at the same time but only half are shipped for an initial phase of construction there is a good probability that the second phase beams will have a higher camber than the first-phase beams. For box and I beam this additional camber may be able to be absorbed by thinning the haunch. Field loading of the field-installed beams to reduce the camber is a method some Contractor's have used to deal with the camber growth. The best methods are for the Contractor to one, order the beams early enough so none of the beams are erected and loaded before they are six months or older, or two, coordinate their and the fabricator's schedules so that the fabricated age of the beams at time of erection is within 30 days of each other for all phases." (OhioDOT 2003)

This research is conducted using two assumptions. Assumption one that elimination of initial differential camber will be sufficient to eliminate differential camber at the time of construction. Assumption two that production scheduling will eliminate wide variance between ages, as well as significant changes in ambient curing conditions of girders, thereby mitigating differences in long term camber growth.

Assuming that steel stress at transfer will be precisely controlled to eliminate variation between members, the concrete will control differences in camber at transfer of prestress. Rigid quality control techniques used by precasters are assumed to eliminate significant variability of member self weight and cross-sectional properties. With previous assumptions in place, initial camber calculations become a function of Young's modulus (E). If prestress transfer for each girder occurs at the same value of E then initial differential camber may be eliminated. If concrete continues to gain strength after transfer at the same rate for all members, then differential camber will be largely eliminated over the storage life of the member. Working with Bayshore Concrete Products of Cape Charles, VA this study seeks to demonstrate the ability to mitigate differential

camber of bridge girders by using concrete maturity as a measure of E and therefore a parameter for transferring prestress.

1.2 - Project Objectives

There are two objectives to this study. The first objective is to develop reliable strength vs. maturity relationships for a standard Bayshore concrete mix design. This will allow strict quality control over release strengths and concrete contributions to camber. The second objective is to study the best techniques for accurately predicting initial cambers, and to apply quality control measures to achieve duplicate cambers on successive girder pours.

This study consisted of two phases of testing. Phase I consisted of laboratory testing to determine the relationship between maturity and strength. Maturity/strength relationships were developed using ASTM C-1074. Materials used in Phase I, were taken from the Bayshore plant stockpiles and were identical to those materials used to produce the concrete mixes for the bridge girders. Phase II consisted of preliminary field tests of girders in production at Bayshore. The girders tested were approach girders to be used by the Virginia Department of Transportation's Route 123 crossing of the Occoquan River in Northern Virginia, United States. During Phase II the following were determined: best location to monitor temperature, correlation between maturity and camber, and other factors contributing to differential camber that require additional study.

1.3 - Project Organization

This paper is organized in the same sequence used in testing. Chapter 2 consists of a review of current methods of camber calculations and maturity methods for estimating strength. The models described in Chapter 2 are used as the basis for testing and analysis used throughout this study. Chapter 3 describes the standard and modified test procedures used in the development of strength vs. maturity relationships as well as, the techniques used in girder testing. Chapter 4 provides test results, as well as analysis used to support conclusions. Chapter 4 is organized in the same sequence used in Chapter 3. Chapter 5 provides conclusions to the hypothesis and research objectives. Chapter 5 also lists recommendations for future research to better understand

parameters of differential camber. Appendix A lists data used in analysis. Appendix B has the shop drawings for girders used in evaluating camber.

Chapter 2 - Literature Review

2.1 - Camber in Pretensioned Concrete Beams

Initial camber at release of pretension is the sum of upward camber and downward deflection due to self-weight. The Precast and Prestressed Concrete Institute (PCI) suggests calculating initial camber by moment area methods, using Youngs Modulus (E) at the time of transfer (PCI, 1999). PCI gives deflection equations for standard prestress strand patterns (PCI, 1999). The PCI camber equations are widely accepted and are used in federal design guidelines (AASHTO, 1998) as well as current textbooks such as Nilson (1987). There are several models used to calculate long-term camber. PCI suggests using multipliers to account for time related effects on long-term camber or deflection (PCI, 1999). Similarly, a more in depth time stepping method is proposed by Nilson (1987). The time stepping method accounts for the time related effects on prestress strand and concrete over a series of small time periods. All long-term camber methods are similar in that they account for the time dependent effects of creep and shrinkage of concrete as well as relaxation of steel. An additional contribution to camber is temperature variation as suggested by Barr, Stanton and Eberhard (Barr et al, 2005). As a pretensioned member is heated during the curing process the differences in thermal coefficients of steel and concrete may lead to a reduction in strand stresses and therefore reduce initial camber by as much as 40% (Barr et al, 2005). This thermal contribution is beyond the scope of this research project. This project focuses on elimination of differential initial camber and will not address long-term effects.

2.1.1. Differential Camber

Initial camber due to prestress is calculated using Equation 2.1 (PCI, 1999), a standard equation for a harped prestress pattern including effect of self weight.

$$\Delta = -\frac{P_o e e l^2}{8EI} - \frac{P_o e'}{EI}\left(\frac{l^2}{8} - \frac{\alpha^2}{8}\right) + \frac{5\omega l^4}{384EI} \qquad \textbf{2. 1}$$

Where: Δ= Midspan deflection, positive down (in)

P_o= Prestress force (k)

e_e= End eccentricity of prestress (in), positive below cg

e'= Harp point eccentricity of prestress (in)

E= Modulus of elasticity of concrete (ksi)

I= Uncracked moment of inertia (in4)

l= Length of girder (in)

α= Length from end to Harp point

ω= Girder self weight, (k/in)

Initial camber variables include geometries of prestressing strand, Young's Modulus and moment of inertia, (I_c). Casting plant quality control will effectively eliminate variation in geometry and moment of inertia by precise placement of reinforcement and use of standard forms. The moment of inertia may be calculated based on the gross concrete section properties as recommended by ACI 318-02 for an uncracked section. Differential initial camber should be reduced to a function of Young's Modulus at transfer of prestress. Research conducted at the University of Texas found a correlation between maturity and Young's Modulus at various temperatures (Kehl et al, 1998). The study also suggested that the use of the maturity method could be a better predictor of member properties than cylinders cured alongside members in a precast plant. Kehl, Constantino and Carrasquillo (1998) found that the temperature of cylinders cured next to a specimen varied by as much as 80^o F from the actual precast members. If Young's Modulus can reliably be predicted at transfer of prestress, then camber may be replicated for members of the same mix design. Currently, transfer of prestress is based on field cured cylinder strengths (AASHTO, 1998).

2.1.2. Modulus Calculation Models

Several models are available for calculating Young's Modulus for concrete. Pauw (1960) suggests a relationship (Equation 2.2) between Young's Modulus, concrete unit weight and concrete compressive strength. Pauw's method is suggested for concrete unit weights between 90

pcf to 155 pcf and compressive strength up to 6000 psi. A second relationship (Equation 2.3) is developed (Carasquillo, et al 1981) for concrete compressive strengths between 3000 and 12000 psi.

$$E_c = 33 w_c^{1.5} \sqrt{f'_c} \qquad \textbf{2. 2}$$

$$E_c = (40{,}000\sqrt{f'_c} + 1{,}000{,}000)\left(\frac{w_c}{145}\right)^{1.5} \qquad \textbf{2. 3}$$

E_c= Youngs Modulus, psi.

f'_c= Concrete Compressive Strength, psi.

w_c= Unit Weight of Concrete, pcf.

2.2 - Maturity Method for Estimating In-Place Strength

2.2.1. Theory, History and Models

Two general observations can be made of concrete. First, concrete compressive strength increases with age. Second, concrete gains strength at a rate proportional to curing temperature. (Mindess and Young, 1981) Maturity is the combination of a time and temperature history. For identical concrete mixes, strength development proceeds with the accumulation of both time and temperature. Therefore, two specimens of the same mix design and with the same accumulation of time and temperature will have approximately the same strength. Measuring maturity allows a strength correlation between specimens with different curing conditions.

In 1951 A.G. Saul was the first to propose a widely accepted concept of maturity (Carino and Lew 2001). Two models dominate current maturity calculation methods. The first model (Equation 2.4) is the Nurse-Saul equation, which is a linear model used to calculate a time-temperature factor (TTF) based on a specimens time-temperature history. The second model (Equation 2.5) was developed in 1977 (Carino and Lew, 2001) and is based on reactions

occurring during hydration of the cement. Equation 2.5, known as the Arrhenius model, accounts for the non-linear relationship between strength and temperature (Carino and Lew, 2001).

$$TTF = \sum_{0}^{t} (T - T_o)\Delta t \qquad \textbf{2. 4}$$

$$t_e = \sum_{0}^{t} e^{-Q\left(\frac{1}{T+273} - \frac{1}{Tr}\right)} \Delta t \qquad \textbf{2. 5}$$

TTF= Temperature Time Factor (^{o}C-hour)
Δt= Time interval between steps, hours
T_o= Datum Temperature, ^{o}C.
T= Average temperature over time period Δt, ^{o}C.
T_r= Reference temperature, Kelvin
Q= Activation Energy divided by the gas constant, Kelvin
t_e= Effective Age, hours

Earlier research (Carino and Lew, 2001) shows the Arrhenius relationship is more accurate for wider temperature variations as may be expected in precast manufacturing. Also, the Arrhenius equation has been shown to be an accurate predictor of early age concrete properties (Okamoto and Whiting, 1994) as would be expected in a precast application. The Arrhenius model calculates an "effective age", which can then be correlated to compressive strength determined from cylinders cured at a reference temperature. Once an "effective age" vs. strength curve is established it can be used to determine strengths for other specimens of the same mix design based on their effective age.

Similarly, Temperature Time Factor vs. strength curves can be used for the Nurse-Saul model. In order to achieve greater accuracy in terms of strength prediction a detailed analysis to determine the appropriate reference temperature and activation energy, used in calculating the effective age, must be conducted in accordance with ASTM C 1074 (Carino and Lew, 2001). The datum temperature used in the Nurse-Saul model is obtained using the same test data used to determine

constants for the Arrhenius equation. Sets of mortar cubes cured in constant temperature baths are used to develop the rate constants for a given mix. Carino and Tank (1992) showed that mortar cubes with a fine aggregate to cement ratio equal to the coarse aggregate to cement ratio used in a concrete mix would follow the same rate of strength gain and could be used to successfully develop maturity constants.

Much of the previously described work has been codified by ASTM C-1074 Standard Practice for Estimating Concrete Strength by the Maturity Method. Annex A of C-1074 formally prescribes the procedures used to develop the constants used in Maturity models. The work of Carino and Tank correlating rate of strength gain for mortar cubes and concrete is used for determining rate constants. C-1074 allows two procedures for determining mortar cube age. The first procedure requires determination of mortar set times and defining age as the difference between actual age and the final set time. The second procedure uses analytical methods using cube compressive strength and actual age. C-1074 also prescribes the thermal recording procedure and minimum standards for developing a Maturity vs. Compressive strength curve.

2.2.2. Maturity Measuring Equipment

Any device that records temperature over a user defined time period is appropriate for measuring maturity. A Type-T thermocouple connected to a data-logger or strip chart recorder works well. In order to reduce the data analysis effort, it is more efficient to have a temperature recording system that can interface with a data analysis computer program. According to ASTM C-1074 temperature must be recorded every 30 minutes for the first 48 hours and 1 hour thereafter. For greater efficiency several commercial "Maturity meters" are available. In general, they can be classified into two categories: stationary thermocouple and data logger with portable reader. The stationary thermocouple system is a data logger, mounted on site and is able to record temperatures from several thermocouples as it continuously calculates the in-place maturity. The portable system (Intellirock, 2004) uses small expendable loggers permanently embedded into the concrete. A portable hand held device is connected to the embedded logger and maturity can be read directly or the temperature history can be transferred to the reader and downloaded into a computer for additional data analysis.

2.3- Significance of Research

Much research has been conducted on the development of the maturity method to predict concrete strength. However, little information is available on the application of maturity in flexural stiffness of early age concrete. This project is a practical application relating maturity to the development of stiffness specifically with respect to modulus of elasticity.

Chapter 3 - Test Procedures

3.1 - Introduction

Testing was conducted in two locations. VPI refers to tests conducted at the Virginia Tech Structures and Materials Lab. BAY also referred to as Field refers to tests conducted at Bayshore Concrete Plant, Cape Charles, VA by Bayshore employees. Material testing was conducted using the same mix design and constituents used in the Bayshore girders. ASTM standard test procedures were followed where applicable. Typically, the rate constants are determined first, followed by the development of maturity curves and finally implementation. However, due to scheduling and resource availability, tests were performed in parallel. The development of the strength/maturity relationship was conducted simultaneously with initial girder tests. Relationships developed from material testing were then applied to actual girder thermal histories to predict girder cambers.

3.2 - Estimating Concrete Strength Using The Maturity Method

Lab tests were conducted to determine relationships between maturity and strength. The basis for testing was ASTM C-1074 with modifications as noted.

3.2.1. Materials

Testing was conducted using a Bayshore standard 8400 psi mix design (Table 3.1). The standard mix typically uses Type III cement. However, some additional testing using Type II was conducted since Bayshore occasionally uses it. NUCEM was used for the slag cement. Daravair was used as the air-entraining agent (AEA). Hycol was used as the water-reducing (WR) agent. Adva was used as the high range water-reducing (HRWR) agent. The use of the WR and HRWR agents were critical in obtaining a workable mixture with a low 0.3 w/c ratio. DCI was used as an accelerating agent as well as acting as a corrosion inhibitor. Plant made batches included DCI as

a portion of the water when calculating w/c ratio. All aggregates were taken from Bayshore stockpiles.

Table 3. 1-Standard concrete mix design
("Pinners Point" f_{ci}=5800 psi, f'_c=8400 psi)

Materials	SSD weights (lb/yd^3)
Portland Cement	510
Slag Cement	340
Coarse Aggregate	1950
Fine Aggregate	988
Water	252
AEA (Daravair)	15 (oz/yd^3)
WR (Hycol)	27 (oz/yd^3)
HRWR (Adva)	175 (oz/yd^3)
C.I. Or Accel (DCI)	4 (gal/yd^3)

3.2.2. Determining Rate Constants

Rate constants used to calculate temperature time factor (TTF) and effective age (t_e) were determined using procedures listed in ASTM C-1074 Annex A. Three sets of tests were conducted. Batch A the first set of tests used Type II cement. Batches B and C the final two sets of tests used Type III cement. For the Type II test (Batch A) an attempt was made to determine set times in accordance with ASTM C-403 using a hand held penetrometer. Due to sporadic results, possibly due to operator error, measurement of set times was abandoned for remaining tests. Alternate analytical methods allowed in ASTM C-1074 Annex A section A1.1.8 were used to calculate constants. Interestingly, the measured final set times for the 50 ^{o}C and the 30 ^{o}C bath were nearly the same. However, the initial set time was nearly an hour later for the higher temperature bath. Applying high curing temperatures immediately after mixing appears to delay set.

The water content of Batch B, the first Type III batch, was reduced to account for the DCI added to the mixture as is done at the batch plant. Batch B was a very stiff and unworkable mix. Batch B rapidly developed large chunks of aggregate and cement, which loosely bonded to one another creating a matrix consisting of large voids in the cubes. The aggregates used in Batch B were

stored outside and were frozen on the day of testing. The aggregates were dried in order to eliminate the ice. The most probable reason for the formation of chunks was that too much oven drying may have dried the aggregates beyond the saturated surface dry condition resulting in some of the water going to saturate the aggregate, leaving too little water to form a paste capable of forming a solid matrix. Also, the low quantity of water used in small batches may be more sensitive to the replacement of water by admixtures. As a result Batch B was discarded due to the lack of consolidation. Batch C the second type III batch consisted of a 0.3 water cement ratio without modification due to the addition of DCI and was a workable mix.

3.2.2.1. Preparing Mortar Batches

Test batches were mixed, placed into standard 2 in. brass mortar cube molds and placed into constant temperature baths for subsequent compressive strength tests. 18 cubes were placed in each of three temperature baths. As specified by ASTM C-1074, the mix design used to determine rate constants was a modification of the standard concrete mix design. The mortar cubes used a fine aggregate to cement ratio equal to the coarse aggregate to cement ratio in the standard concrete mix design. The mortar mix used the same water to cement ratio and admixture to cement ratio as the standard concrete mix. Water was added at ambient temperature 20-24 ^{o}C. The mortar cube mix proportion, without modification of the amount of water due to DCI, is given in Table 3.2 for one set of 18 cubes.

Table 3. 2: Mortar Cube mix

Materials	SSD weights (lb)
Portland Cement	3.49
Slag Cement	2.32
Fine Aggregate	13.33
Water	1.74*
AEA (Daravair)	3.1 ml
WR (Hycol)	5.4 ml
HRWR (Adva)	35 ml
C.I. Or Accel (DCI)	104 ml

Mix design for 18-2 in. cubes
*w/c=0.3 not reduced by admixture liquid volumes

Batch A was mixed in a 2.5 ft^3 bread mixer. Batch A was used to produce eighteen, three cube sets, and six-6in. x 6in. x 6in specimens for measuring set times. The fines and cement were placed into the mixer in two layers, each consisting of half the cement and half the fines. The dry ingredients were mixed for two minutes to ensure uniform distribution. The water was added followed by the admixtures and the batch was mixed for an additional two minutes. The mortar cubes were placed on a vibrating table in sets of four to six, filled with mortar, troweled smooth and removed from the vibrating table after troweling was complete. In order to delay set, the mixer continued to run while filling mortar cubes. A total of thirty minutes elapsed from the time water was added until the last molds were filled. Within fifteen minutes of adding water the mortar mix became stiff and difficult to work in the mixer. However, when vibrated the mix became workable and adequate consolidation was achieved. Batch C was made in three smaller batches (C1, C2, C3) one each for high, medium and low temperature curing. Because these batches were smaller, they were easily molded prior to set. Each batch was mixed in a five-gallon pail mixer, following the same procedure as Batch A except mixing was stopped while filling the cube trays. Each batch produced six sets of three cubes as well as three additional cubes in case the initial test strength was too low and must be conducted again at a later age.

3.2.2.2. Curing Mortar Cubes

The six sets of three cubes as well as specimens used to determine set times for Batch A, were placed into three constant temperature baths (Figure 3.1); a hot bath of 50 ^oC, a warm bath of 30 ^oC and a cold bath of 10 ^oC. The hot and warm baths consisted of enclosed, insulated thirty gal. plastic tubs encased in a wooden shell. The baths were heated with aquarium heaters and water was circulated with an aquarium pump. The pump operated constantly, while the heating elements were controlled by a MICROMEGA CN77000 Series Controller, using a type-T thermocouple, set with a tolerance of 1 ^oC within the specified temperature. The cold water bath was a 100 gal enclosed tank with cooling coils around the perimeter. The cooling tank uses a constant temperature thermostat with a tolerance of 2 ^oC. All water baths were saturated with hydrated lime in accordance with ASTM C-511 to saturate the water and prevent additional hydration by the bath water. All mortar cubes for a given curing temperature were removed from their forms one hour prior to the first strength tests and returned to the bath.

Figure 3. 1: Curing Bath with OMEGA temperature controller

3.2.2.3. Mortar Cube Strength Tests

Initial strength tests for Batch A (Type II) were performed at an age of twice the final set times. Set times were found using penetration tests in accordance with ASTM C-403. Penetration tests gave final set times of 8.5 hr for the cold bath and 10.3 hr for both the hot and warm bath. The unusually low set time for the cold bath was discarded and initial tests were conducted at 21.5 hr. Human error or a false set may have accounted for the error. Due to the difficulty of measuring set times, this method was abandoned for the subsequent batches.

For Batch B (Type III) the first hot cubes were tested at 12 hr and based on their low strength additional testing was delayed until 24 hr. Warm and cold cube tests were performed at later ages on the assumption that strength gain would develop more slowly due to lower curing temperature. Based on the large number of defective cubes, due to improper consolidation, Batch B was abandoned. However, based on the accumulated data from Batch B, initial test times were determined for Batch C. Based on rates of strength gain for Batch B the warm bath appeared to be the most predictable. The hot bath cubes had a very high rate of strength gain, but it was difficult to predict when the rapid strength gain would begin. The cold bath cubes gained strength too slowly to make subsequent testing efficient. Initial tests were to be conducted when cube strength reached 580 psi. A linear interpolation from the Batch B cubes indicated an initial test time of 11.5 hr should work for batch C cubes cured at 30 ^{o}C.

Batch C was made of three smaller batches C1, C2, and C3 each made at different times. Each batch consisted of six sets of three cubes for strength testing as well as one additional set of three cubes to refine the initial testing time. Batch C1 was placed into the warm bath (30 ^{o}C). One cube was tested at 10.5 hr with a strength of less than 580 psi. At 11.5 hr a second cube was tested and exceeded 580 psi. Additional tests were performed at twice the age of the previous test in accordance with ASTM C-1074 Annex A.

Batch C2 was placed into the hot bath (50 ^{o}C). Based on past experience cubes placed in the hot bath reached final set more slowly than the warm bath. Based on the idea that a delay period prior to high temperature curing is necessary to allow initial hydration and therefore improve stability (Mindess) the C2 batch was left at room temperature for one hour following molding, then moved to the warm (30 ^{o}C) bath for two additional hours prior to going into the hot (50 ^{o}C) bath. Based on cumulative temperature and time for the warm cubes, an initial test time was calculated as eight hours for the hot cubes. One hot cube was broken at 8 hr and was less than 200 psi. A second test was performed at ten hours. Using the 8 and 10 hr. test values and assuming linear strength gain up to 500 psi a third test time was calculated as sixteen hours. At 16 hr. the hot cubes had only reached 400 psi. A fourth test was conducted at 20.5 hr resulting in adequate strength for initial testing.

The higher curing temperature appears to delay initial strength gain. For future study final set times should be measured if possible and used to determine initial test ages. In lieu of testing set times, it should be expected that higher curing temperatures begin strength gain later than warm cured (20-30 ^{o}C) specimens. ASTM C-1074 Annex A recommends testing cubes at twice the age of the previous test for example 12hr, 24hr, 48 hr. Due to rapid strength gain from high temperature curing, an accelerated test schedule was used for the hot cubes. An interval of approximately five hours was used to ensure adequate data points within the rapid strength gain phase.

Batch C3 was placed into the cold bath (10 ^{o}C). Using data from the warm bath tests an equivalent cumulative temperature and time was used to predict an initial test time for the cold cubes, and refined based on test cubes.

For all strength tests, cubes were pulled from their bath, dried and allowed to set for ten minutes prior to testing. Cubes were placed on a cube pedestal, centered and tested in a Forney compressive strength machine. Three cubes were broken and compressive strengths averaged. If a cube showed signs of defect, its test was discarded. Also, if one of the cube's tested strength was off by more than 10% of the average strength, it was discarded as well. All cube test data is provided in Appendix A-2.

3.2.3. Development of Strength versus Maturity Curves

Maturity versus strength curves for concrete cylinders were developed using compressive strength versus some measure of maturity. Similar curves were also established for elastic (Young's) modulus versus maturity. Three batches were produced at the VPI lab. All batches were proportioned based on the standard Bayshore mix design Table 3.1. Batches VPI-0 and VPI-1 used Type II Portland Cement. Batch VPI-2 used Type III Portland cement. Two batches BAY-1 and BAY-2 were produced in the field at Bayshore's batch plant, both used Type III Portland Cement. In addition to the cylinders being tested to develop maturity relationships, each set of girders had a set of field cure cylinders cast to determine release strength, as well as to provide 7 day and 28 day strengths, as required by the Virginia Department of Transportation (VDOT). These cylinders undergo the same casting, curing and testing as BAY-1 cylinders, however maturity was not directly measured for the girder field cured cylinders. Maturity for the field cured cylinders was estimated to be the same as the girder they were closest to.

3.2.3.1. Preparing Concrete Batches

Batches prepared at the VPI lab used the standard one-yard mix design proportions, modified for smaller batches depending on the number of cylinders required for testing. Portions were measured and dry ingredients were mixed for two minutes followed by the addition of water, then admixtures. The batch was mixed in a 2.5 ft^3 bread mixer for two minutes following addition of admixtures. The batch continued to mix while being cast into 4 in. x 8 in. plastic mold cylinders in accordance with ASTM C-192. Slump and air content were measured

immediately following the two minute mix time. Cylinders prepared in the field were taken directly from the batches used in the girders and cast, by certified Bayshore QC technicians, into 4 in. x 8 in. plastic molds. For each test batch temperature, recording loggers were inserted into the center of selected cylinders and activated within 30 minutes from the time water was added to the mix.

3.2.3.2. Curing Concrete Cylinders

Moist cure cylinders at the VPI lab were cured in a moist room which maintained relative humidity of 95% or greater. Humidity was obtained by a forced air constant mist system. The moist room was kept at a temperature of 20 ^{o}C to 23 ^{o}C. Cylinders remained in plastic molds for seven days or until tested, whichever occurred first. Moist cure cylinders at Bayshore were cured inside capped cylinder molds at a constant temperature of 23 ^{o}C. The molds remained capped until testing in order to mitigate moisture loss. High temperature cured cylinders at the VPI lab were cured in the same 50 ^{o}C bath used for mortar cubes. Match or field cure refers to cylinders cast and cured under the same conditions applied to test girders. Match cured cylinders were capped to eliminate moisture loss and placed on racks attached to girder forms located at the point farthest from the steam input. After release the cylinders were placed in outdoor racks located near the QC lab, but not adjacent to the girders. For VPI-0, all 29 cylinders were moist cured. VPI-1 had 8 cylinders moist cured, 9 cylinders hot cured and 8 cylinders were cured hot for 20 or more hr. and randomly transferred to moist cure conditions. For VPI-2 10 cylinders were moist cured and 5 cylinders were cured at 50 ^{o}C for 24 hr. then transferred to moist cure to replicate the match cure process used for girders.

3.2.3.3. Concrete Cylinder Strength Tests

Strength tests conducted at VPI were performed using a hydraulic pump operated Forney compression testing machine. Cylinders were capped with neoprene pads for testing. Sulfur caps were used in 14 day and later tests, since neoprene pads were inadequate at these higher strengths. Strength tests conducted at Bayshore were performed by qualified QC technicians using a Hobart CRT compression testing machine, and neoprene pad caps. For all strength tests

the ultimate strength of two cylinders were averaged. If the cylinder strengths varied by more than 10% a third cylinder was broken, and the cylinder with the largest error with respect to the three-cylinder average was rejected.

Cylinder test times were selected to develop a series of data points describing strength development over 28 days with some data concentration in the 4000 psi to 7000 psi range. Using cumulative temperature and time versus strength from Bayshore moist cylinders cast with BAY-1 on December 17,2004, VPI-2 test times were selected (Table 3.3). However, based on rapid early strength gain, the test schedule was accelerated.

Table 3. 3: Concrete cylinder test schedule

Batch	Cement Type	Curing	Test interval, f_c	Test interval, E
VPI-0	II	Moist	64h, 72, 80, 89, 4d, 6, 14, 26	64h, 72, 80, 89, 4d, 6, 14, 26
VPI-1	II	Variable	39h, 48, 56, 4d	39h, 48, 56, 4d
BAY-1	III	Accelerated	16h, 24, 64, 6d	None
VPI-2	III	Moist	24h, 72, 4d, 5, 8, 14, 28	72h, 4d, 5, 8, 14, 28

3.2.3.4. Concrete Cylinder Modulus Tests

Elastic modulus was determined for select mixes in order to study the accuracy of existing models and to describe the relationship between modulus and maturity. For a given test age, cylinder ultimate strengths were found and an upper limit of 40% of ultimate strength was used to evaluate modulus. Test cylinders were placed in neoprene pad caps and a digital compressometer with an accuracy of 0.00005 in. was attached (Figure 3.2). The gage length was measured at 5.25 in. and the cylinder was carefully centered within the diameter of the compressometer. The cylinder was placed into a Forney compression testing machine. The load was applied at approximately 40 psi/sec up to the maximum test load. The compressometer was checked following the initial loading cycle to ensure it was properly seated. Two to three

subsequent loading cycles were performed and measurements recorded for calculation of Young's Modulus. During each load cycle an initial gage reading was taken at 2000 lb when using the low range load gage and 5000 lb for high range, and as the load approached the maximum test load the highest gage reading was recorded just prior to releasing the applied load. The dial indicator on the compression testing machine provided the highest applied load. Strain was calculated as $\varepsilon = \frac{d}{2(5.25)}$ where d is the dial reading from the compressometer. The compressometer used was a digital readout, which could be zeroed before each test and therefore did not require an initial reading. Young's modulus was calculated as the slope of the best-fit linear expression for a plot of stress versus strain for each data point (Figure 3.3). Cylinder weights were recorded for each batch an average unit weight of 156 lb/ft^3 was calculated. The average unit weight is used with existing mathematical models to calculate Young's Modulus based on compressive strength.

Figure 3. 2: Compressomter used to measure Elastic Modulus

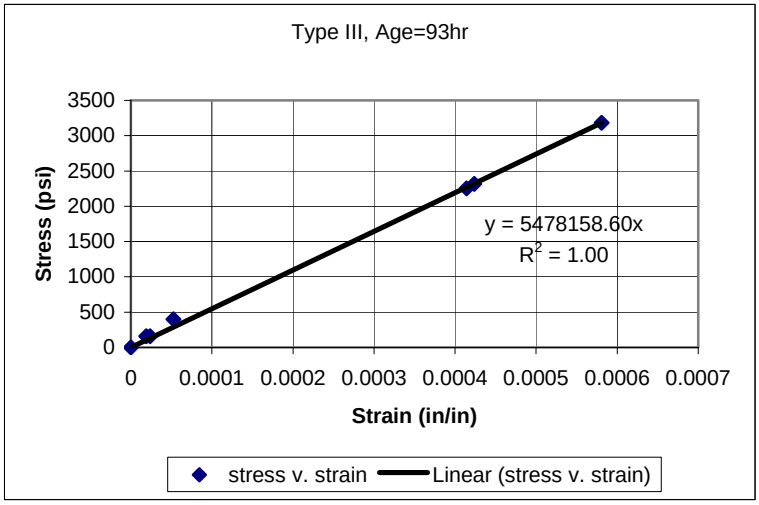

Figure 3. 3: Typical Modulus test results

3.3 - Girder Tests

Girder tests were conducted on 144 ft. long VDOT standard PCBT-77 girders with a harped tendon profile. Typical prestress arrangement included 0.6 in. diameter 270 ksi low relaxation strand with a profile of 34 straight strands with 6 harped over the middle 10,000 mm or 32.8 ft. giving an end eccentricity of 23.4 in. and a harping point eccentricity of 33.1 in. The prestress jacking force is specified as 44.3 k/strand. Shop drawings for the girders poured on can be found in Appendix B (metric units). Of the seven girders tested five were identical, and two poured on 1/5, were similar, but had slightly different lengths and used fewer strands. Temperature histories and camber at transfer were measured to determine the relationship between concrete maturity and initial camber. Girders were cast in 300 ft open beds. One pour consisted of two girders, which will be denoted as North and South. The steam pipes approach the bed at mid length and split to both ends running along the east side of the bed. The steam was piped to distribution pipes with perforations to allow steam application, see Figure 3.4. Tarps were placed over the girders to hold the steam over the girder enabling uniform curing temperatures along the curing bed

3.3.1. Maturity Measurement

Figure 3. 4: Curing bed with steel layout, and steam distribution pipes located at base of bed.

Bayshore Concrete Cape Charles, VA

Temperature histories were recorded using Intellirock data loggers. The data loggers were pre-programmed by the manufacturer to take readings at 30 min for 28 days. The first pair of girder tests on December 17, 2004 were used to understand temperature gradients through the depth and length of the girder as well as to understand variations within the bed. The initial girder tests also provided data on the relationship between girder temperature histories and cylinders cured next to the girders. Loggers were placed in the top flange, the web and within the bulb at midspan of the southern girder to determine variation through the depth of the girder. Loggers were placed in the top flange and bulb at the southern end to compare the variation along the length of the girder. One logger was placed in the bulb of the northern girder to determine variation of within the bed. One logger was also placed with the field cure cylinders BAY-1 to understand the relationship between field cure cylinders and the actual girders. Loggers were placed at selected locations (Figure 3.5) and secured with standard metal wire ties along the length of the data logger cable (Figure 3.6). For the second girder test January 5, 2005, loggers were placed in the bulb at midspan of both girders. An additional logger was placed in the top flange of the southern girder for comparison.

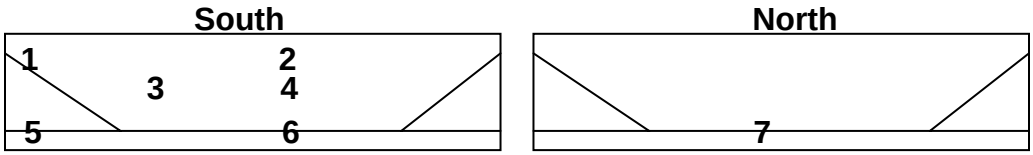

Figure 3. 5: Location of temperature recorders December 17, 2005. Field cure cylinders at location 3 opposite steam lines.

Figure 3. 6: Intellirock data logger attached to confining steel (location 5) at the end of the girder.

3.3.2. Camber Measurement

Cambers were measured for the seven girders described in the previous section. All camber measurements were taken by Bayshore personnel. Camber measurements were taken twice. Immediately after release, camber was measured on the bed with a tape measure and using the bed as the reference datum. Camber was taken a second time following movement of the girders to their storage location within the yard. Girders were placed on dunnage at the bearing locations of the girders. Standard surveying instrumentation was used to establish a datum by measuring elevations at the ends of the girders and taking the datum as half the difference in end elevations. Elevation at midspan was then measured. Camber was taken as the difference between the midspan elevation and the datum line established from the two end elevations.

Chapter 4 - Results and Analysis

4.1 - Introduction

This chapter presents results of lab and field tests and measurements. Rate constants were determined based on results of mortar cube tests conducted at the Virginia Tech lab (VPI). Curves relating maturity to Young's Modulus (E) and strength (f_c) were developed in the VPI lab and compared to field cylinders. Girder tests provided temperature histories and camber measurements at transfer. Field cured cylinder strengths were also measured at transfer. Actual girder cambers were compared against calculated cambers using stiffness properties based on maturity.

4.2 - Maturity Method Strength Estimates

Maturity equations require rate constants in order to relate variable curing temperatures to the maturities of "standard" moist cure cylinders. The Nurse-Saul equation (Equation 2.4) uses a datum temperature T_o and the Arrhenius equation (Equation 2.5) requires a constant Q equal to the activation energy divided by the Gas Constant. Compressive strength tests of mortar cubes cured in a range of constant temperature baths provide the data to calculate the maturity constants. Using ASTM C-1074 Annex A1.1.8 rate constants were calculated based on curing temperature, age and cube compressive strength.

4.2.1. Maturity Function Constants

The ultimate strength S_u for the mortar cubes was calculated as the inverse of the y-intercept for a best-fit plot of 1/Strength along the y-axis plotted against 1/Age along the x-axis, as shown in Figure 4.1 where age is referenced to the time water was added to the mortar mix. Relative strengths were determined for the first four test ages (App. A: Table A2.2). Relative strength is defined as A=S/(Su-S) where S is the compressive strength at each test age. A-values were

plotted against age for each curing temperature, as shown in Figure 4.2. The slope of the best-fit line for each temperature is the K-value. K-values are given in Appendix A Table A-2.3 for Type III and Table A-2.7 for Type II. K-values are then plotted against temperature and the y-intercept determines T_o (Figure 4.3). Q is the negative of the slope from a plot of Ln(K) plotted against 1/Temperature (Kelvin) (Figure 4.4). Maturity constants are summarized in Table 4.1. Similar figures for the Type II mix are presented in Appendix A Tables A-2.4 to 2.7 and Figures A-2.5 to 2.9.

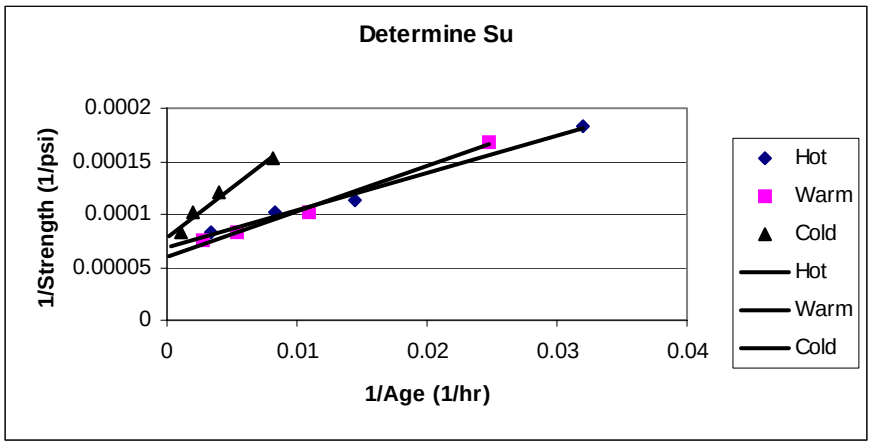

Figure 4. 1 (Type III mix, Su)

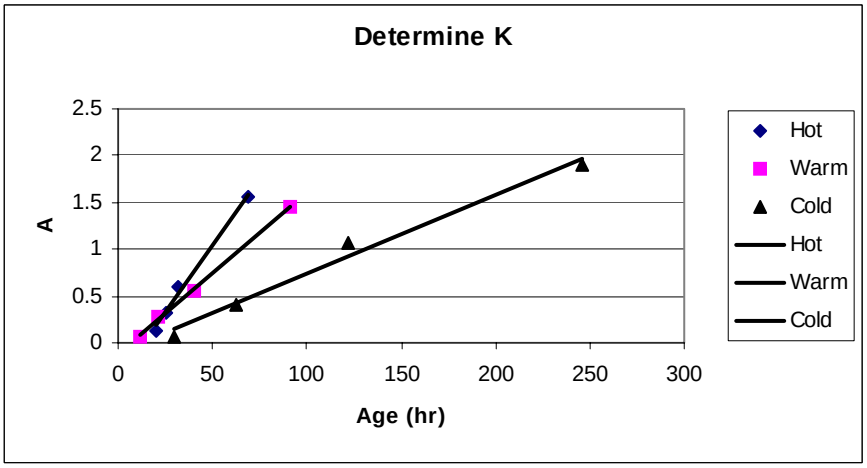

Figure 4. 2 (Type III mix, K)

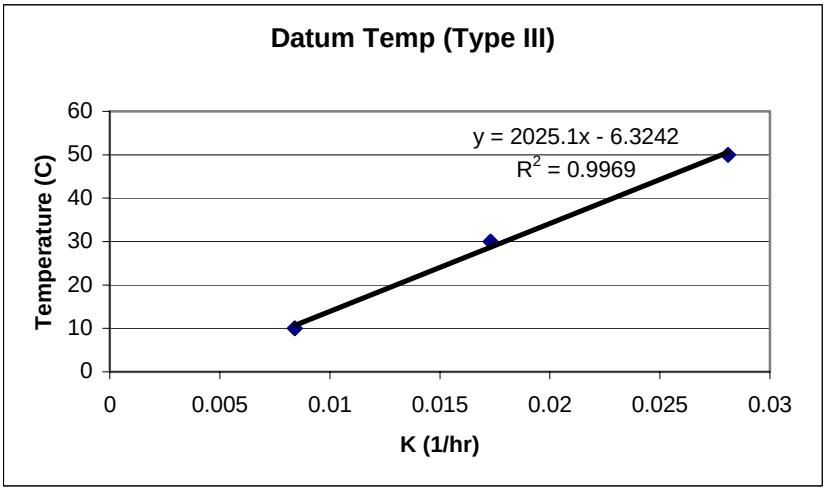

Figure 4. 3 Datum temperature T_o=-6^{o}C (T_o =y-intercept)

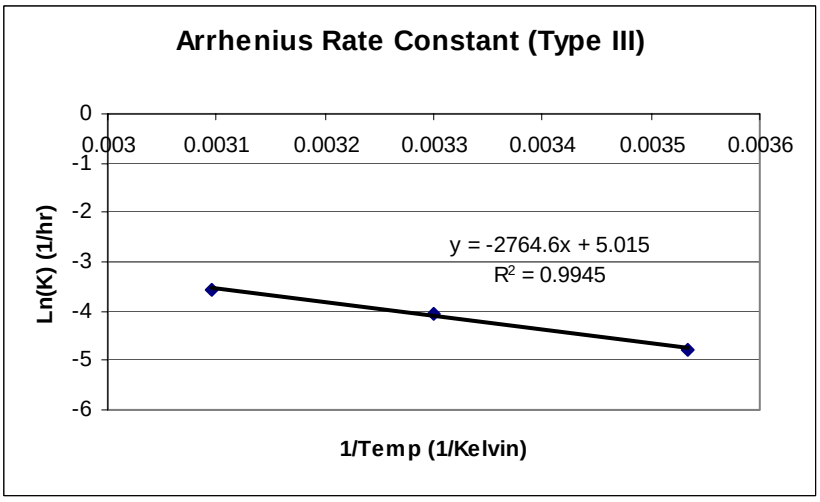

Figure 4. 4 Q=2760 (Q=Slope)

Table 4. 1: Maturity Rate Constants

	T_o(^{o}C)	Q(Kelvin)
Type II	-1	3410
Type III	-6	2760

Rate Constants (Ref: Appendix Figures A 2.8, 2.9 for Type II graphs)

4.2.2. Maturity Models

4.2.2.1. Strength Models

Maturity curves were developed using both the temperature time factor (TTF) and effective age (t_e). Comparisons were made to determine the best models for predicting strength. Models were generated using best-fit equations for the "standard" moist cure strength vs. maturity plots. For example Equation 4.1 is the quadratic best fit model using the effective age maturity method for the Type III mix. The two types of equations considered were logarithmic and quadratic. Models were analyzed in the maturity ranges typical of prestress transfer times. These models are not recommended for t_e>150 hr. or TTF>3500^{o}C-hr, the quadratic model is especially sensitive to larger values of maturity where calculated strengths will decrease after the parabolic function reaches it's maximum value.

Models were compared based on three criteria: precision, accuracy and efficiency. Precision was used to evaluate the most effective mathematical model as the model that best fit the data. Accuracy was used to evaluate the most effective maturity model as the model which most accurately predicted strength of accelerated cure cylinders. Efficiency is defined as the model requiring the least amount of calculation effort.

The first criterion, precision is measured by R-squared values for best fit "trend lines" for the "standard" moist cure cylinder data. Results of the analysis are given in Table 4.2. All models had very good R-squared values, greater than 0.98; however, the quadratic models Equations 4.1,

4.2, 4.5 and 4.6 were slightly more precise than the logarithmic models Equations 4.3, 4.4, 4.7 and 4.8. Only the quadratic model will be analyzed for accuracy. Figure 4.5 shows a graphical representation of the relationship between the Log best fit model and the moist cure cylinder test values used to develop the curve. The graphical analysis for the remaining models are presented in Appendix A Figures A-3.1 to 3.8.

The second criterion was accuracy as measured by the residuals between the "best fit" model and actual values of strength for accelerated cure cylinders. Error was calculated by the square root of the sum of squares (SRSS) method. Strength values were calculated, using the quadratic best-fit equation models for both the temperature time factor and the effective age maturity methods, for accelerated cure cylinders. The residual is the difference between the actual test strength of accelerated cure cylinders and the calculated model strength.

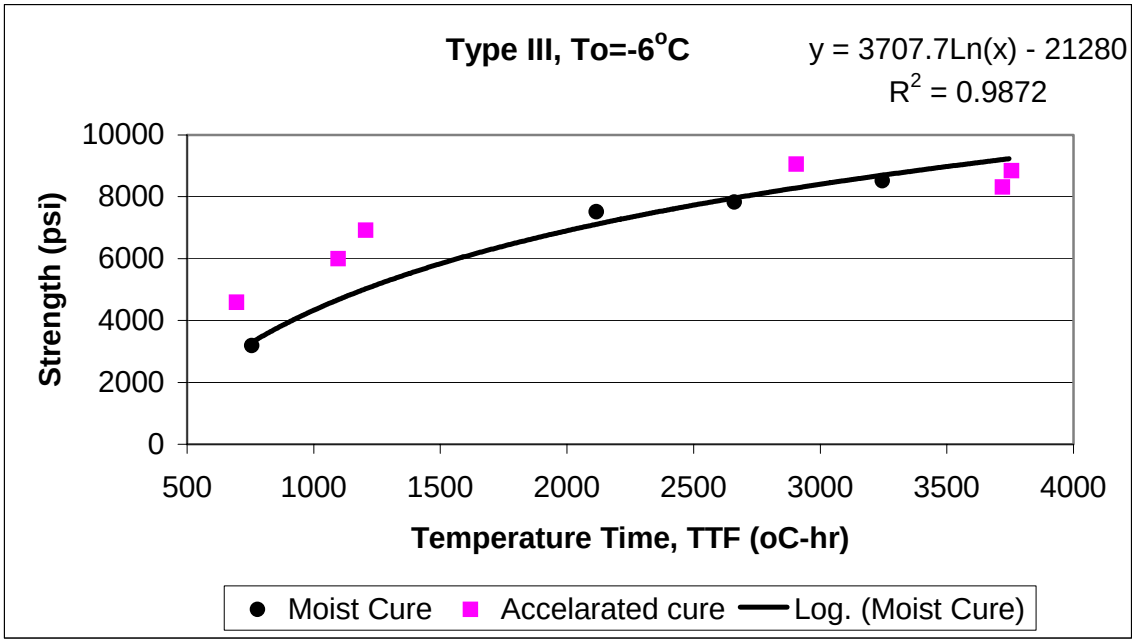

Figure 4. 5: Relationship between model curve and actual test values for accelerated cure cylinders. The equation given is the best-fit logarithmic model based on moist cure cylinder strengths.

The residual was then squared and summed for each model. The complete analysis is given in Appendix A Tables A-3.3 and 3.4. A summary of results for the SRSS analysis is given in Table 4.3. Figure 4.5 graphically illustrates the accuracy for a given maturity model by showing the difference between accelerated cure cylinder tests and the model curve. The larger SRSS values are in greater error and therefore less accurate. The error is highest for the Type II Effective Age model. The remaining models have similar SRSS values. Normalizing the results of the SRSS analysis to the lowest value of 2680 for the effective age model, results in values of 1.01 and 1.13 for the Type II and III TTF models respectively. The normalized values for the effective age model are 1.87 and 1 for the Type II and III respectively. Due to the lack of a clear trend the most accurate model is taken as the Temperature Time Factor maturity model since it appears to be the most reliable having similar accuracy for both the Type II and Type III mix. Quadratic models are given below in Equations 4.1, 4.2, 4.5 and 4.6. Logarithmic models are given in Equations 4.3, 4.4, 4.7 and 4.8. All strength data is listed in Appendix A: Table A-3.1 and 3.2.

Type III: (T_o=-6°C; Q=2760 K)

$$f_c = -0.0008TTF^2 + 5.37TTF - 371 \quad \textbf{4.1}$$

$$f_c = -0.602t_e^2 + 145t_e - 338 \quad \textbf{4.2}$$

$$f_c = 3710Ln(TTF) - 21300 \quad \textbf{4.3}$$

$$f_c = 3690Ln(t_e) - 8940 \quad \textbf{4.4}$$

Type II: (T_o=-1°C; Q=3410 K)

$$f_c = -0.0013TTF^2 + 10.0TTF - 10900 \quad \textbf{4.5}$$

$$f_c = -0.926t_e^2 + 267t_e - 10700 \quad \textbf{4.6}$$

$$f_c = 7940Ln(TTF) - 56400 \quad \textbf{4.7}$$

$$f_c = 7910Ln(t_e) - 30100 \quad \textbf{4.8}$$

Where: f_c= Compressive strength in psi

TTF= Temperature Time Factor °C-hr

t_e= Effective Age in hr

Table 4. 2: Summary of R^2 values for Strength

R^2 (Equation)		Ln	Quad.
Type II	TTF	0.981**(4.7)**	0.999 **(4.5)**
	te	0.981**(4.8)**	0.998 **(4.6)**
Type III	TTF	0.987 **(4.3)**	0.993 **(4.1)**
	te	0.987 **(4.4)**	0.992 **(4.2)**

Analysis of model Precision: Results of R^2 analysis of logarithmic and quadratic models for "standard" moist cure strength vs. maturity.

Table 4. 3: Summary of SRSS results for strength

S.R.S.S.		Quad.
Type II	TTF	2700
	te	5010
Type III	TTF	3020
	te	2680

Strength model accuracy analysis by SRSS method

The third criterion was defined as ease of use. The calculation effort was used in determining the easiest model to work with. The temperature time factor is the easiest measure of maturity to use. The Intellirock temperature recorders give real time temperature time factors and therefore on site decision making is possible. The logarithmic model is the easiest model to work with. Fewer calculator keystrokes are required to calculate strength. Calculating the maturity required to reach a defined strength requires solution of a quadratic equation for the quadratic model. The practical example below illustrates the calculating effort to determine the maturity required (M_{rqd}) to achieve a desired strength f_c=6000 psi. This application would be typical for a precaster trying to determine when to transfer prestress force.

Ln model: $f_c=7943*Ln(M)-56397$ → find Maturity required $M_{rqd}=e^{(6000-(-56397))/7943}$

Quadratic model: $f_c=-0.0008*M^2+7.28*M-7318$ → find Maturity required M_{rqd}= solution to quadratic $-0.0008*M^2+7.28*M+(-7318-6000)=0$

Based on the three criteria: the most precise model is the quadratic equation; the most accurate model is the Arrhenius model using effective age, t_e; the easiest model is the logarithmic using TTF. With no clear best model for strength prediction any model is acceptable. For fieldwork the logarithmic model using t_e if measured directly is the best prediction model. If t_e cannot be

measured directly, the TTF logarithmic model is acceptable. For the remaining analysis the quadratic model using TTF (Equation 4.1) will be used based on the superior fit of the quadratic model and the ability to directly measure TTF.

4.2.2.2. Modulus Models

Modulus testing was only performed on VPI batch cylinders. Maturity vs. Modulus curves were developed using "standard" moist cure cylinders. Logarithmic and quadratic best-fit equations were determined for each method of measuring maturity. Model comparison is conducted using the same criteria defined for the strength models. R-squared values were used to determine the most precise "best fit" mathematical model for predicting Modulus based on maturity. The maturity model accuracy was determined using the SRSS method on the residuals comparing modulus calculated using the best fit models given below as Equations 4.9 to 4.16 for both maturity measures (TTF, te) with cylinder modulus test values for accelerated cure cylinders. The R-squared values are all acceptable with the lowest value being 0.944 for the Type III logarithmic model (Table 4.4). All other model comparisons are presented in Appendix A Figures A-3.13 to 3.16. The most precise model is clearly the quadratic model.

Accuracy analysis is limited due to the lack of data for the Type III mix. Only one modulus value was measured within the maturity range of interest for the Type III mix (Table 4.5). The accuracy for that range of maturity appears to be similar for both Type III and Type II mixes.

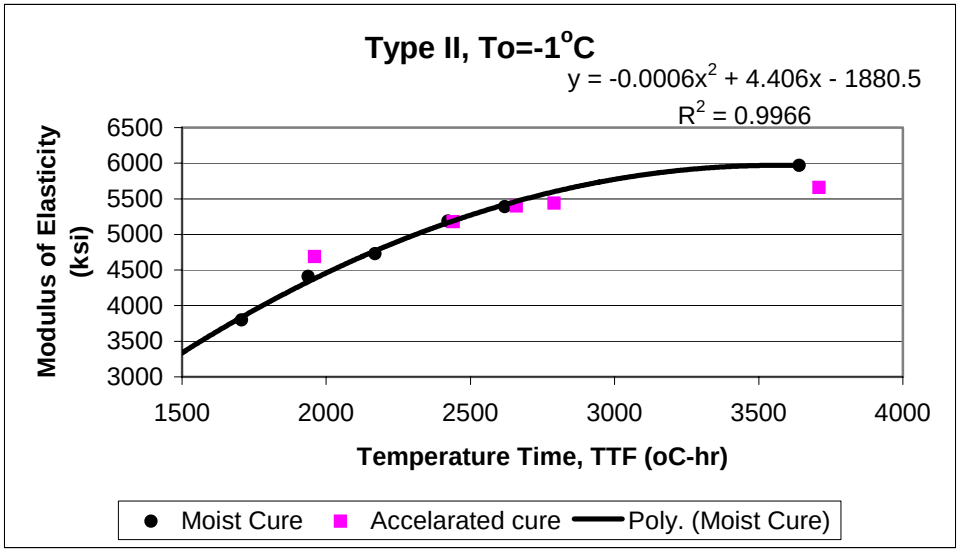

Figure 4. 6: Relationship between model curve and actual test values for accelerated cure cylinders. The equation given is the best-fit quadratic model based on moist cure cylinder modulus.

Type III: (T_o=-6°C; Q=2760 K)

$$E_c = -0.0001TTF^2 + 1.34TTF + 2870 \quad \textbf{4. 9}$$

$$E_c = -0.101t_e^2 + 35.8t_e + 2910 \quad \textbf{4. 10}$$

$$E_c = 1065Ln(TTF) - 2980 \quad \textbf{4. 11}$$

$$E_c = 1060Ln(t_e) + 571 \quad \textbf{4. 12}$$

Type II: (T_o=-1°C; Q=3410 K)

$$E_c = -0.0006TTF^2 + 4.41TTF - 1080 \quad \textbf{4. 13}$$

$$E_c = -0.446t_e^2 + 118t_e - 1830 \quad \textbf{4. 14}$$

$$E_c = 2830Ln(TTF) - 17000 \quad \textbf{4. 15}$$

$$E_c = 2820Ln(t_e) - 7670 \quad \textbf{4. 16}$$

Where: E_c= Modulus of Elasticity in ksi

TTF= Temperature Time Factor ^{o}C-hr

t_e= Effective Age in hr

Table 4. 4: Summary of R2 results for Modulus models

	R^2	Ln	Quad.
Type II	TTF	0.951	0.997
	te	0.953	0.998
Type III	TTF	0.944	0.997
	te	0.944	0.997

Table 4. 5: Summary of SRSS results for Maturity Modulus models

Cement	Maturity	SRSS
Type II	TTF	724
	te	1328
Type III*	TTF	649
	te	620

*Only one data point available E=4470 ksi at TTF=1970^{o}C-hr or t_e=78.2 hr

Analysis of model accuracy was therefore based solely on the Type II mix data and then used ot select the best model to apply to the Type III mix. The most accurate prediction of modulus is based on maturity measured by the temperature time factor with the lowest SRSS value in Table 4.5. The effective age model is not accurately predicting modulus gain with maturity and is in fact unconservative as shown by Figure 4.8 where V-C represents variable (accelerated) cure and M-C represents constant temperature moist cure. Based on the previous analysis of precision and the results if the accuracy analysis, the quadratic model using TTF for the maturity parameter is the best model for predicting modulus. All models are valid only up to the largest value of tested maturity and should not be used for prediction beyond that limit. For calculating modulus for 1000 ^{o}C-hr<TTF<3500 ^{o}C-hr the Equation 4.9 may be used for the Type III mix. A conservative underprediction may occur for TTF<1500 ^{o}C-hr.

A comparison was also made between modulus as calculated using equation 4.9 and values calculated using typical strength based models, Equations 2.2 and 2.3. Figure 4.8 shows that equation 4.9 is conservative at lower maturities typically found at transfer.

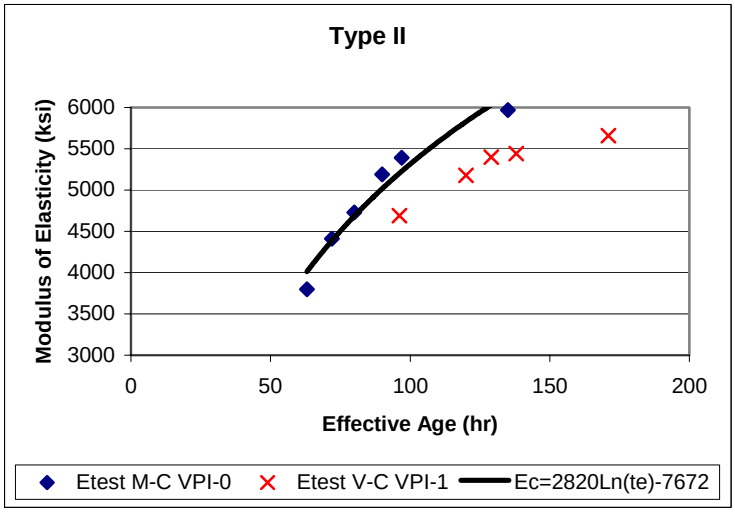

Figure 4. 7: M-C is moist cure cylinders;
V-C is variable (accelerated cure)

Additional testing should be conducted to determine the accuracy of the strength-based models against the maturity-based model. Recommended study would be to generate another "standard moist cure" Maturity vs. Modulus curve with 6-8 data points ranging from 1000 ^{o}C-hr<TTF<3500 ^{o}C-hr and compare to tested and calculated values of Modulus for field cured cylinders.

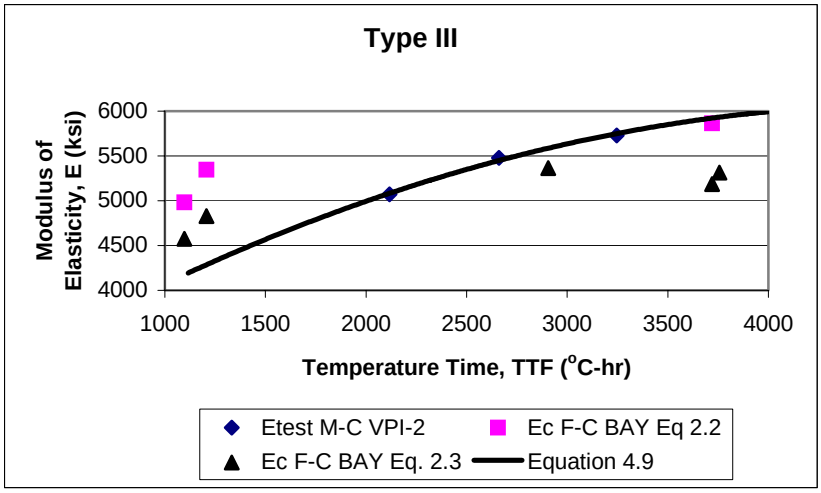

Figure 4. 8: Comparing E(Maturity) to E(f'c) Field Cure where F-C is field (accelerated) cure.

4.2.3. Girder Maturity Measurements

Results of the first girder test December 17, 2004 clearly show that temperature and maturity vary through the depth of the girders (Figure 4.9). As expected the bulbs, points 6 and 7 in Figure 3.5, generate a higher heat due to hydration of the cement. Maturity measured at the ends of the beam were 6 and 10% lower than midspan maturities for girders poured on 12/17/04 and 2/16/05 respectively. (Appendix A Table A-4.1) The impact of the lower maturity values for girder ends was to decrease the modulus by 2 to 3%. The small impact on modulus has a negligible affect on camber. Cylinders cured alongside of the girders did not achieve temperatures as high as the girder during the steam-curing phase. For the first girder test, cylinder maturity at transfer was about 10% lower than the girder bulbs. (Table 4.6)

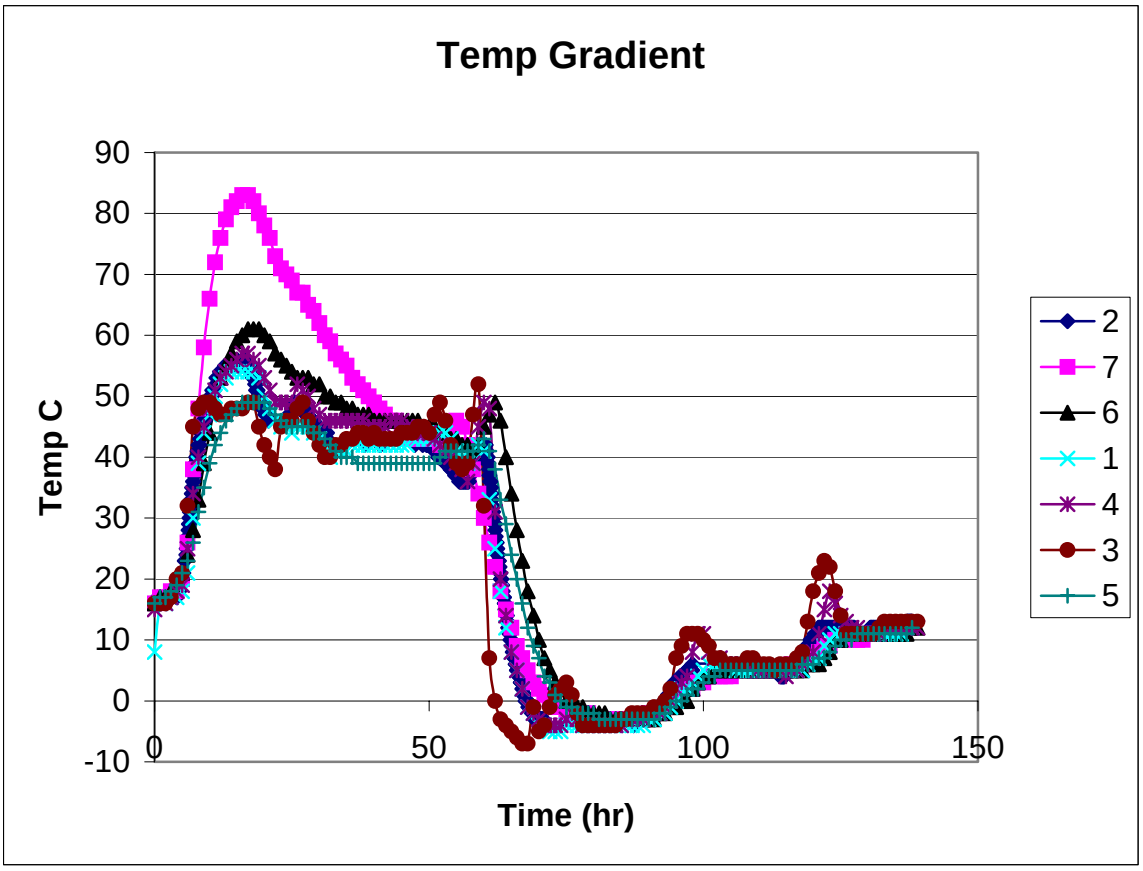

Figure 4. 9: Temperature history for Girder test December 17, 2004. Location referenced by Figure 3.5.

Table 4. 6: Maturity at various locations within girders poured 12/16/04. Maturity measured at 24 hours. Reference location by Figure 3.5

Location	1 (top)	2 (top)	3 (cyl.)	4 (mid)	5 (bulb)	6 (bulb)	7 (bulb)
Maturity (^{o}C-hr)	1130	1150	1100	1180	1300	1200	1560

4.3 - Girder Camber

Girder camber measured immediately after transfer was significantly different from camber measured following movement. Bed cambers averaged ½ in. where cambers after movement were typically between 1 ½ and 2 ½ in. The friction between the girder and bed apparently contributes a significant longitudinal restraining force reducing camber. All cambers used in analysis were taken following movement to storage. Shop drawings specified a prestress force of

44.3 k/strand or approximately $0.75f_{pu}$ for 270 ksi strand. Although strand forces were not measured during testing Bayshore QC manager described standard procedure as overjacking to account for relaxation losses thereby providing the specified prestress force of 44.3 k/strand at release.

4.3.1. Calculation models and results

Camber was predicted using equation 2.1 where E was determined using one of three methods. The first method was to calculate E using both equation 2.2 and 2.3 where field cured cylinder strengths were used for f_c. The second method was to calculate E using equation 2.2 and 2.3 where f_c was calculated based on maturity using equation 4.1. The third method was to calculate E using equation 4.9 where E is a function of maturity. Values of E varied as much as 20% between methods. (Table 4.8)

Elastic shortening was calculated using f_{cs}, the stress at the centroid of prestressing strand, at midspan. Elastic shortening was taken as the change in stress (or force) between jacking and transfer of prestress force. Typical losses were approximately 10% as shown by Table 4.7. The variation between the elastic shortening losses calculated by equation 4.17 using the various values of concrete modulus could be significant.

$$ES\% = \frac{\left(\frac{E_p}{E_c}\right) * f_{cs}}{f_{pj}} \qquad \textbf{4. 17}$$

Where:

E_p= Prestress modulus of Elasticity 27,0000 ksi

E_c= Concrete modulus of Elasticity at transfer

f_{cs}= Stress at centroid of prestress strand

f_{pj}= Jacking stress (206 ksi)

As shown by Table 4.7 the calculated elastic shortening loss for the 12/17 pour is nearly 45% less than the 2/16 pour. This is a worst case, but it it's a typical production scenario where release does not occur at the desired maturity. For other cases where transfer occurs at the same

maturity the difference in elastic shortening losses between girders is minimized. For example the elastic shortening loss of prestress force is only 1% less for the 4/11 pour when compared to the 2/16 pour. Complete list of elastic shortening losses for all variations of E is presented in Appendix A Table A-4.3

Using standard Bayshore procedures, steel relaxation was mitigated by measuring jacking force at the live (pulling end) of the strand prior to detensioning. Relaxation is not added into prestress loss calculations. However as a reference, a prestress loss of 2% results in approximately a 1/16 in. decrease in camber.

Table 4. 7: Elastic Shortening losses for various locations and girders. Pj taken as 44.3 k/strand; Pe is force after shortening. E taken from Equation 4.9.

Location-Girder	x (ft)	e (in)	L (ft)	P_j (k)	$E_c(t)$	ES loss (%)	P_e (k)
end 12/17 South	0	23.4	143.33	1772	6660	-5%	1680
harp 12/17 South	55.3	33.1	143.33	1772	6660	-7%	1640
midspan 12/17 South	71.7	33.1	143.33	1772	6660	-7%	1640
mid 12/17 North	71.7	33.1	143.33	1772	6770	-7%	1650
mid 1/5 North	68.6	33.4	137.2	1506	4300	-10%	1360
mid 1/5 South	71.9	33.4	143.8	1506	4350	-10%	1360
mid 2/16 North	71.7	33.1	143.33	1772	4420	-11%	1580
mid 2/16 South	71.7	33.1	143.33	1772	4420	-11%	1580
mid 4/11 South	71.7	33.1	143.33	1772	4200	-12%	1570

4.3.2. Comparison Between Calculated and Actual Camber

A comparison between calculated and actual cambers is provided in Table 4.8. Modulus values and cambers calculated as described in section 4.3.1 above. The girders poured 1/5/05 had a different prestress arrangement using only 34 strands and having slightly different lengths. The camber measurements taken 1/5/05 are questionable as they are more than two times the predicted value. Since camber measurements were taken by Bayshore, it is difficult to determine the cause of the large difference. For all other pours the most reliable prediction of camber is calculated using equation 4.9 to predict the modulus and then using that value of E to calculate the elastic shortening loss and the resulting camber. With the exception of the girders poured on 1/5/05 and 4/11/05 all predicted cambers are within 1/4 in. of the measured camber. The

tolerance for measurement is 1/8 in. The 4/11/05 girders calculated camber underestimated the camber by ½ in. Maturity for the 4/11 girders was measured at transfer. However, the camber wasn't measured until six days later, so some camber growth due to shrinkage and creep could have occured. Figure 4.10 illustrates the accuracy of the predictive methods. By plotting measured camber against the various predicted camber methods, it is easily seen that the use of the maturity modulus function is the best fit lying along the 1:1 standard line. The north girder consistently has a lower camber, which is likely due to a variation in heating within the bed. Equation 2.2 underpredicts modulus compared to Equation 2.3.

Table 4. 8: Calculated and measured camber for north and south girders, listed by pour date. E(ksi), Camber (in.)

	N. 12/17/04	S. 12/17/04	N. 1/05/05	S. 1/05/05	N. 2/16/05	S. 2/16/05	S. 4/11/05
Maturity TTF ^{o}C-hr	4250	4030	1170	1210	1270	1280	1080
E1A= *fn* ($f_{c,cyl}$) Eq 2.2	5990	5990	5330	4980	5390	5340	4980
E1B= *fn* ($f_{c,cyl}$) Eq 2.3	5240	5240	4780	4540	4820	4790	4540
E2A= *fn* ($f_{c,Mat}$) Eq 2.2	5700	5790	4420	4480	4580	4580	4270
E2B= *fn* ($f_{c,Mat}$) Eq 2.3	5040	5100	4150	4200	4260	4270	4050
E3= *fn* (Mat)	6770	6660	4300	4350	4420	4420	4200
Camber *fn* (E1A)	1 5/8	1 5/8	1 3/8	1 3/8	1 7/8	1 7/8	2
Camber *fn* (E1B)	1 7/8	1 7/8	1 1/2	1 3/8	2	2	2
Camber *fn* (E2A)	1 3/4	1 3/4	1 1/2	1 1/2	2	2	2 1/8
Camber *fn* (E2B)	2	1 7/8	1 1/2	1 5/8	2 1/8	2 1/8	2 1/4
Camber *fn* (E3)	1 1/2	1 1/2	1 1/2	1 5/8	2 1/8	2 1/8	2 1/4
Camber Measured	1 3/8	1 1/2	2 7/8	3 3/8	2	2 1/8	2 1/2

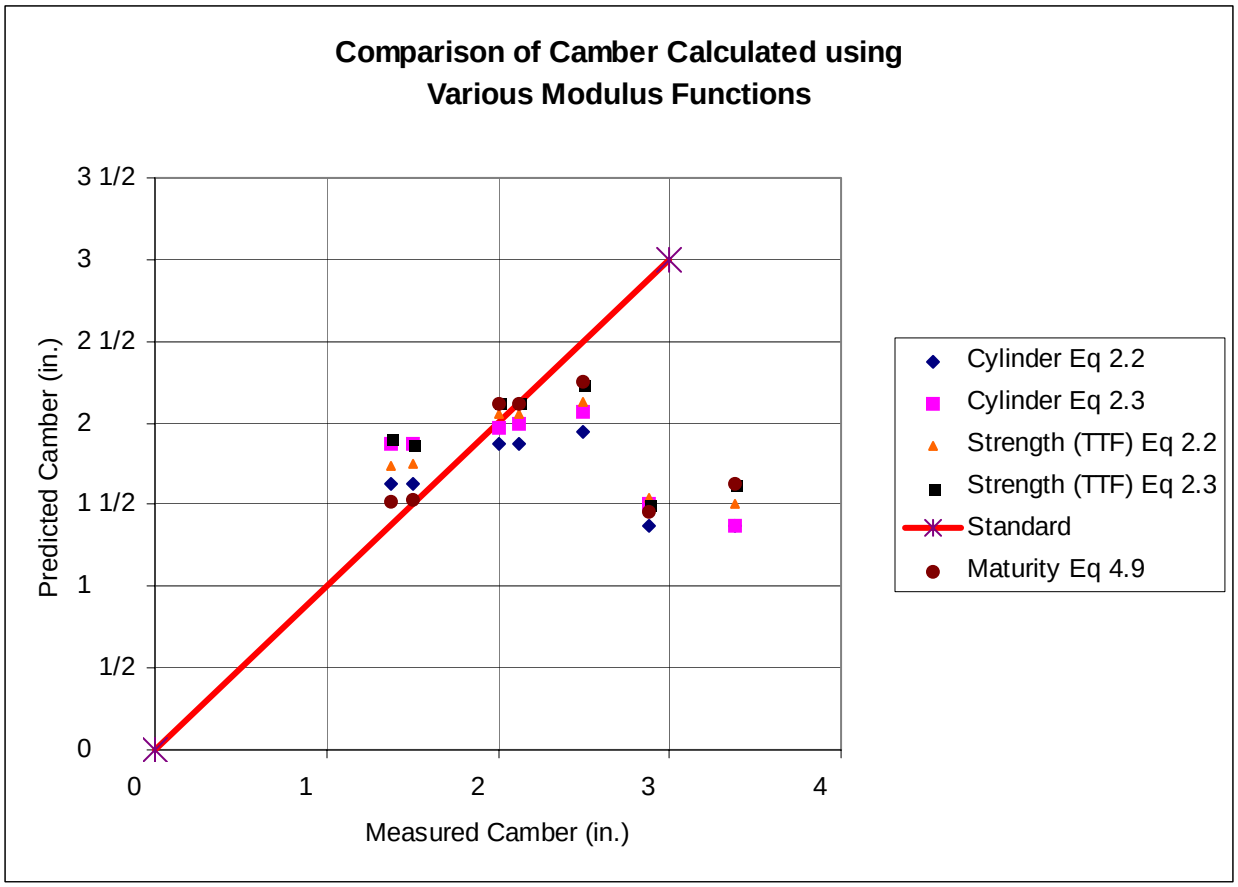

Figure 4. 10: Comparison of camber predictions using data from Table 4.8

Chapter 5 - Conclusion and Recommendations

5.1 - Using Maturity to Eliminate Differential Camber

The use of Maturity clearly offers a means to accurately tie the desired design camber to the actual achieved camber in production. Camber would typically be predicted based on an established minimum cylinder compressive strength at transfer of prestress. As shown in Table 4.8 the difference between camber calculated using cylinder strength and that using maturity can be as much as ½ in. or 25%. And differences in the actual cylinder release strength can vary depending on the curing cycle. By specifying the camber or modulus in the design process the precast manufacturer can use his maturity function as a quality control measure to produce an actual member with the same specifications as the designed member. Using the maturity parameter offers a valid quality control method to mitigate initial camber variations

5.2 - Advantages of Using Maturity in a Precast Environment

Using maturity in a precast environment will enable producers to efficiently use curing energy. By specifying the required maturity and using environmental temperature forecasts the steaming period can be accurately tailored to achieve the desired strength at the optimal time in the scheduling of labor. Use of ambient temperatures can be used to significantly reduce unneeded curing energy while still ensuring the required strength will be achieved by the desired time for prestress transfer. The need for multiple cylinder breaks can be eliminated by using Maturity as the transfer parameter and breaking cylinders only as confirmation of strength. Maturity is a better indicator of girder strength than cylinders and may eventually be accepted as a standard in lieu of cylinder tests. It must be noted that the use of maturity requires strict adherence to quality control on batch characteristics affecting strength. If parameters such as the water/cement ratio or air content is varied the maturity will not accurately predict concrete strength parameters.

5.3 - Disadvantages of the Maturity Method

Development of a maturity curve is time consuming and difficult. Initial labor will be very expensive to establish curves. For jobs requiring a special tailored mix the maturity method is not economically advantageous over cylinder strength methods. However, for mixes that are routinely used the development of a maturity function would be advantageous. The cost of temperature recording devices can make the maturity method uneconomical. At nearly $40 for the intellirock recorders used in this study the cost of maturity measurement is not advantageous for small inexpensive jobs.

5.4 - Additional Study Required

5.4.1. Affect Curing Cycle Variation

The girder tests for this study were typically done on similar curing cycles where concrete was poured late afternoon, steam was applied overnight and transfer occurred the following morning at approximately 18 hr. Additional study is required to determine if the same level of accuracy can be achieved using curing cycles with minimal energy input such as a weekend pour.

5.4.2. Sensitivity of Mix Variation

A parametric study of the impact of various concentrations of admixtures and the affect of varying the proportions of cementitious material, such as slag, to the amount of Portland cement would offer insight into the sensitivity of maturity rate constants to the concrete mix composition.

5.4.3. Crossover Affect

The crossover affect as defined by the decreased ultimate strength of concrete cured at elevated temperatures compared to the same concrete cured at typical temperatures of around 20 ^{o}C requires additional study. By studying a large number of specimens cured under various

conditions an additional fitting parameter may be able to account for the variation with curing cycle.

5.4.4. Long term Camber affects

Study of the long-term camber growth is needed to prove the validity of initial assumptions that long term camber growth due to creep and shrinkage will be similar. Will the crossover affect significantly impact the long-term camber for members with similar initial maturity values?

References:

Pauw, Adrian , “Static Modulus of Elasticity of Concrete as Affected by Density,” ACI Journal, Proceeding V. 57, No. 6, Dec. 1960, pp.679-687

Carasquillo, R. L., Nilson, A.H., and Slate, F.O., “Properties of High Strength Concrete Subject to Short Term Loads,” ACI Journal V. 78. No.3, 1981, pp 171-178.

Slate, F.O., Nilson, A.H., and Martinez, S., “Mechanical Properties of High Strength Lightweight Concrete,” ACI Journal V. 83. No.4, 1986, pp 606-613.

Carino, N. J., and Lew, H.S., “The Maturity Method: From Theory to Application,” Proceedings of the 2001 Structures Congress and Exposition, Washington D.C., May 2001, p.19

Kehl, R, Constantinos, C and Carrasquillo, R., “Investigation of the Use of Match Cure Technology and the Maturity Concept as New Quality Assurance Measures for Concrete,” Center For Transportation Research, University Of Texas At Austin, August 1998

Schindler, A., “Effect of Temperature on the Hydration of Cementious Materials,” Harbert Engineering Center, Auburn University, Auburn, AL

Okamoto, P.A., and Whiting, D. “Use of Maturity and Pulse Velocity Techniques To Predict Strength Gain of Rapid Concrete Pavement Repairs During Curing Period,” Transportation Research Record, No. 1458, National Academy Press, Washington, D.C. 1994,pp. 85-90

Carino, N. J., and Tank, R.C., “Maturity Functions for Concrete Made with Various Cements and Admixtures,” ACI Materials Journal, Vol 89, No. 2, March-April 1992, pp.188-196

Intellirock, 2004 website www.intellirock.com

AASHTO LRFD Bridge Construction Specification (1998). American Association of State Highway and Transportation Officials, Washington, D.C.

PCI Design Handbook (1999). Precast/Prestressed Concrete Institute, Chicago, IL

Mindess, Sidney and Young, J Francis (1981). Concrete, Prentice Hall, Englewood Cliffs, NJ

Nilson, Arthur H. (1987). Design of Prestressed Concrete, John Wiley and Sons, New York, NY

Barr, P.J., Stanton, J.F., Eberhard, M.O., "Effects of Temperature Variations on Precast, Prestressed Concrete Bridge Girders," Journal of Bridge Engineering, Vol 10, No 2, March-April 2005, pp. 186-194

Ohio DOT, 2003 website
http://www.dot.state.oh.us/construction/OCA/Specs/2002CMS/2003_Manual_for_web/515.htm